



HAL
open science

Dynamics of a Cambered A320 Wing by Means of SMA Morphing and Time-Resolved PIV at High Reynolds Number

Mateus Carvalho, Cédric Raibaud, Sébastien Cazin, Moïse Marchal, Gilles Harran, Clément Nadal, Jean-François Rouchon, Marianna Braza

► To cite this version:

Mateus Carvalho, Cédric Raibaud, Sébastien Cazin, Moïse Marchal, Gilles Harran, et al.. Dynamics of a Cambered A320 Wing by Means of SMA Morphing and Time-Resolved PIV at High Reynolds Number. 5th Symposium on Fluid Structure Sound Interactions and Control, FSSIC 2019, Aug 2019, Chania, Greece. pp.283-293, 10.1007/978-981-33-4960-5_44 . hal-03602466

HAL Id: hal-03602466

<https://hal.science/hal-03602466v1>

Submitted on 9 Mar 2022

HAL is a multi-disciplinary open access archive for the deposit and dissemination of scientific research documents, whether they are published or not. The documents may come from teaching and research institutions in France or abroad, or from public or private research centers.

L'archive ouverte pluridisciplinaire **HAL**, est destinée au dépôt et à la diffusion de documents scientifiques de niveau recherche, publiés ou non, émanant des établissements d'enseignement et de recherche français ou étrangers, des laboratoires publics ou privés.

Dynamics of a cambered A320 wing by means of SMA morphing and time-resolved PIV at high Reynolds number

Mateus Carvalho^{1,2}, Cédric Raibaudo³ Sébastien Cazin, Moïse Marchal, Gilles Harran, Clément Nadal, Jean-François Rouchon, and Marianna Braza

¹ LAPLACE, Laboratoire Plasma et Conversion d'Énergie,
Toulouse 31000, France

`carvalho@laplace.univ-tlse.fr`

² IMFT, Institut de Mécanique des Fluides de Toulouse,
Toulouse 31000, France

³ ONERA, Toulouse 31000, France

Abstract. A great deal of current scientific and technological advances in aeronautics concerns innovative wing design in order to increase aerodynamic performance, it is normal to seek better efficiency and refinement for critical structures. Inspired from the nature, deformations and vibrations are applied to aircraft wings. Thanks to smart-materials that deform a structure, an electroactive morphing wing prototype at reduced scale has been realized within the Smart Morphing and Sensing project. Force measurements show that electroactive morphing increase lift up to 2% with wake thickness reduction of around 10%. High-speed time-resolved particle image velocimetry reveals important effects on flow dynamics as well as on time average. Based on these results, this paper proposes the experimental study of the influence of a Shape Memory Alloy (SMA) actuator on the dynamics of a reduced scale A320 wing by means of time-resolved PIV. The velocity fields obtained are analyzed using Proper Orthogonal Decomposition and reconstruction of the dynamic system is performed to identify coherent structures present at the flow...

Keywords: aerodynamics, turbulence, PIV, closed-loop control, morphing, wind-tunnel experiments, smart materials

1 Introduction

It is well known that presently airfoil shapes are not designed to optimize the aerodynamic performance in all flight phases, but still the drag-lift ratio of an aircraft must vary depending on the flight state. Since it has been a major matter of interest in aeronautical industry, recent studies [1] show that camber control of the trailing edge may be a solution to reduce aircraft operational costs. Adapting the shape of the wing during the flight can save several percent of fuel consumption for a commercial aircraft. Such concept is called morphing

and it has been of extensive research for more than 40 years [1]. The concept of morphing aims to optimize drag-lift ratio by means of shape modification in order to adapt the flow in real time.

The main inspiration for this project is the nature. It has been proven that some species of fish are able to manipulate surrounding turbulence to reduce muscle activity [2]. Going even further, owls have an unique mechanism to reduce noise during flight [3]. All of these aspects can and should be used to enhance the performance of aircrafts. It is not a simple task though. Conventional electromechanical actuators are not the most suitable way to achieve shape optimization mostly because of cost, weight and complex mechanical integration [1]. These issues have motivated recent advances in the field of smart materials such as shape memory alloys (SMA) and piezoelectric macrofiber composites (MFC). Smart materials provide sufficient stiffness to withstand the aerodynamic loads, while being flexible enough to be deformed, showing the potential to be an alternative to conventional electromechanical actuators [4, 5].

Considering electroactive materials, Shape Memory Alloys (SMA) and piezoelectric materials are commonly used. SMA are characterized by thermomechanical behaviors, and most of the applications use actuation by means of Joule heating. Typical applications are shape adaptation at low deformation speed. Piezoelectric materials are activated when exposed to an electric field. Piezoelectric composites are suitable from low to very high frequencies and allow easy integration with electrodes.

Electroactive morphing has been the focus of a partnership between LAPLACE and IMFT laboratories for more than 15 years in various collaborative research projects. For the Smart Morphing and Sensing (SMS) European project an electroactive reduced scale prototype has been realized. This prototype embeds both SMA and piezoelectric macro fiber composites (MFC). SMAs ensure high deformation, around 10% of the chord, for camber control while MFCs perform deformation of the trailing-edge at higher frequencies up to 400Hz [6]. Wind tunnel experiments show that piezoelectric MFC actuation reduces the energy of the wing's wake thanks to an interaction between the vibrating trailing-edge and the shear layer [7].

Following previous work, [7, 8], the first section of the article is dedicated to the design of the reduced scale prototype. The second section introduces the wind tunnel experimental setup, used to perform force measurements and High Speed Time Resolved Particle Image Velocimetry (HS TR-PIV). The following sections show experimental results obtained after hybrid morphing (SMA and MFC actuation) and present the perspectives for the SMS project.

2 Prototype Description

The considered prototype is an electroactive hybrid morphing wing. It embeds both camber control and Higher Frequency Vibrating Trailing Edge (HFVTE) actuators. The baseline airfoil is a wing section of an A320. The chord is 700 mm and the span 590 mm. This aspect ratio affects the flow, but it does not affect the

actual results, as the experiments are dedicated to the changes in the flow due to morphing compared to a non-morphing wing. Fig.1 presents the prototype and its three different sections. The actuators are sized, simulated and implemented on the last 30% of the chord, corresponding to usual flap positions. The hollow fixed leading edge contains electronics and tubing for all temperature, pressure and position transducers as well as actuator interfaces.



(a) RS Prototype [9]



(b) Prototype actuated section

Fig. 1: Reduced scale prototype developed by Laplace and IMFT.

The camber control actuators working principle relies on distributed structure embedded actuators: SMA wires are spread under the upper and lower aluminum skins of the wing. The actuation of the upper wires (suction side) causes bending of the trailing edge towards higher cambered shapes. Antagonistically, the actuation of SMA wires under the pressure side skin causes a decrease in camber. Figure 1b shows the SMA actuated wing section. The selected wires are made of Nickel and Titanium. Their properties are activated by a change in temperature. They are heated thanks to electric current through themselves. When warmed, the wires tend to retract by a 3% strain that have been previously trained. The modification between martensite and austenite phase in the material internal structure generates a change from plastic to elastic regime, so the SMA tend to recover the initial length. The SMA actuators are designed to support the aerodynamic loads corresponding to a Reynolds number equal to 1 million, which corresponds to a flow velocity of 21.5 m/s in IMFT wind-tunnel. They are able to generate intense stress of more than 600 MPa under these large

deformation levels. These materials have been studied for decades, Lexcellent provides an accurate SMA handbook [10].

The HFVTE actuators are composed of metallic substrates sandwiched between "Macro Fiber Composite" (MFC) piezoelectric patches on both sides. MFC patches are LZT piezoelectric fibers and electrode networks encapsulated within epoxy. When supplied by a voltage, the patches stretch out and generate bending. The whole is covered by a flexible molded silicon that gives the trailing edge shape. Figure Fig.2 illustrates the actuator topology. The active length of the HFVTE is 35 mm chordwise. Push-push actuators are also seen in literature for this purpose [6]. This design allows for quasi-static tip deformation peak to peak amplitude on the order of 2 mm, while able to vibrate at amplitudes large enough up to 400 Hz. The authors invite the reader to refer to the previous publications [8,9] for more details related to the design and the electromechanical characterization of this electroactive morphing wing.

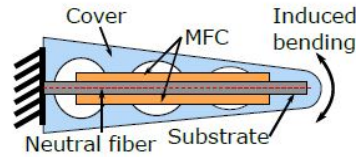


Fig. 2: HFVTE actuator.

3 Experimental Set-up

The experiments were performed in the IMFT (Institut de Mcanique des Fluides de Toulouse) wind-tunnel. The test section is 592 mm width per 712 mm high. The prototype is mounted at an incidence of 10° . As a result a blockage ratio of 18% is obtained, which is considered acceptable in these experiments. The turbulence intensity of the inlet section is about 0.1% of the free stream velocity. Measurements are carried out at ambient temperature (22°C).

PIV campaign was performed to investigate the influence of the SMA actuation on the flow. In order to image both the upper and the lower surfaces of the wing a 400mm Nikon lens was chosen. Indeed, as shown in Fig.3, the experimental set-up of this campaign, the 3 meters distance between the camera and the test section of the wind tunnel reduces the parallax effect. It was then necessary to use a flexible mask to avoid direct laser reflection on the prototype surface. Furthermore, to Particle images are recorded at a rate of 5 kHz using a digital high-speed camera Phantom V2012. The laser sheet is generated by a Photonics DM60-527-DH. 0.5m particles were employed to obtain an investigation window size of 170 per 260 mm. The commercial software DaVis10 from LaVision was used for post-processing.



Fig. 3: PIV equipment. Configuration used to to image both upper and lower surfaces of the wing.

4 Results

The PIV campaign was performed at Reynolds number of 1 million in which corresponds to a flow velocity of 21.5 m/s in the IMFT wind-tunnel. The high speed camera recorded a sequence of snapshots of the SMA actuation of the prototype. The trailing edge comes from static position, that means no actuation performed, to full cambered position in about 1.5 seconds.

The first step for the analysis of the experimental results was to plot the streamtraces of the snapshots obtained with the PIV campaign. It is a fast and useful tool to understand the flow dynamics. In Fig.4 one can see the snapshots corresponding to the static position and the full cambered case. As it is expected there is an increase in the recirculation zone such as in take-off and landing configurations of commercial aircrafts.

A monitor point was chosen in the lower shear layer in the wake of the wing. The normalized coordinates in relation to the chord of the wing are $x/c = 1.14$ and $y/c = -0.20$. Then the power spectral density of the two velocity components were calculated. The results are shown in Fig.5. They are consistent with numerical simulation results obtained [11] where the frequency of von Kármán instabilities were found to be around 120 Hz in the lower shear layer region.

4.1 POD Analysis

The Proper Orthogonal Decomposition is a mathematical method used to detect the coherent structures featured by the flow based on their wake number and frequency. It allows us to understand the flow behavior by finding the so-called POD modes that form the dynamic system. This approach is largely used in the analysis of experimental data [12,13] and numerical simulation. The reader can find a more detailed description of the POD in [14].

In Fig.6(a) we see the POD modes ranked by their energy. In the case of full camber position, higher modes have more energy than in the static case.

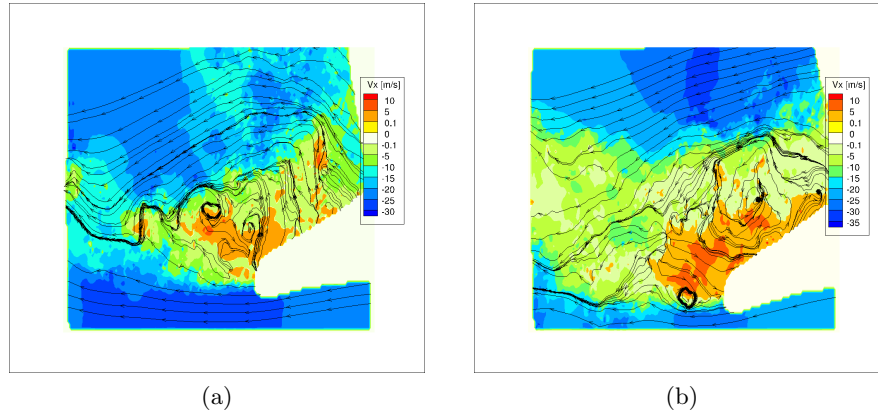


Fig. 4: Streamtraces from PIV campaign. (a) No morphing, (b) full SMA actuation.

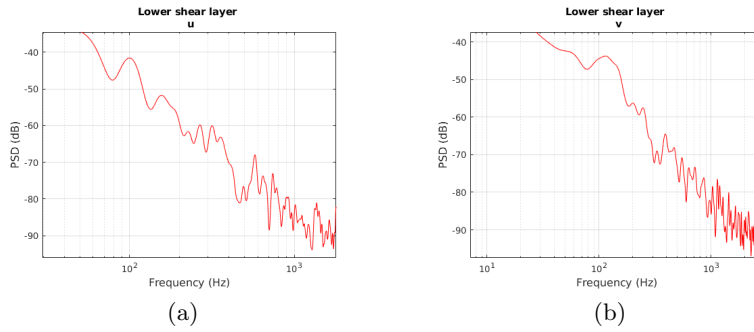


Fig. 5: PSD of monitor point in the shear layer. (a) and (b) correspond to the position ($x/c = 1.14$, $y/c = -0.20$)

One can see it clearly in Fig.10 were the PSD of the temporal coefficients of the modes 3 and 5 are presented for static and cambered cases. The rise of the energy can be explained by the increase of big coherent structures during SMA actuation. In general, we need more POD modes to describe the dynamics of the flow around the cambered wing, as it is shown in Fig.6(b). Since the recirculation zone is larger, beyond the big energetic vortices, more small structures are formed which correspond to less energetic modes (Fig.9).

The dynamics of the flow are reined by big structures inside the recirculation zone. Fig.7 and Fig.8 show the modes 3 and 5 respectively. In both figures we see an augmentation of the vortices after SMA actuation which is consistent with the results obtained with PSD analysis and energy rank.

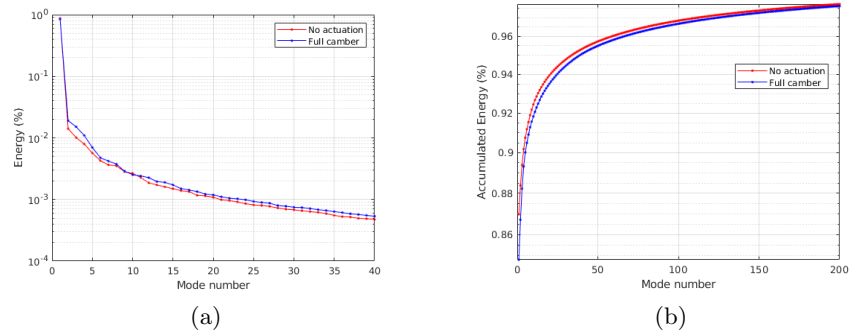


Fig. 6: Comparison between: (a) energy from POD modes and (b) accumulated energy.

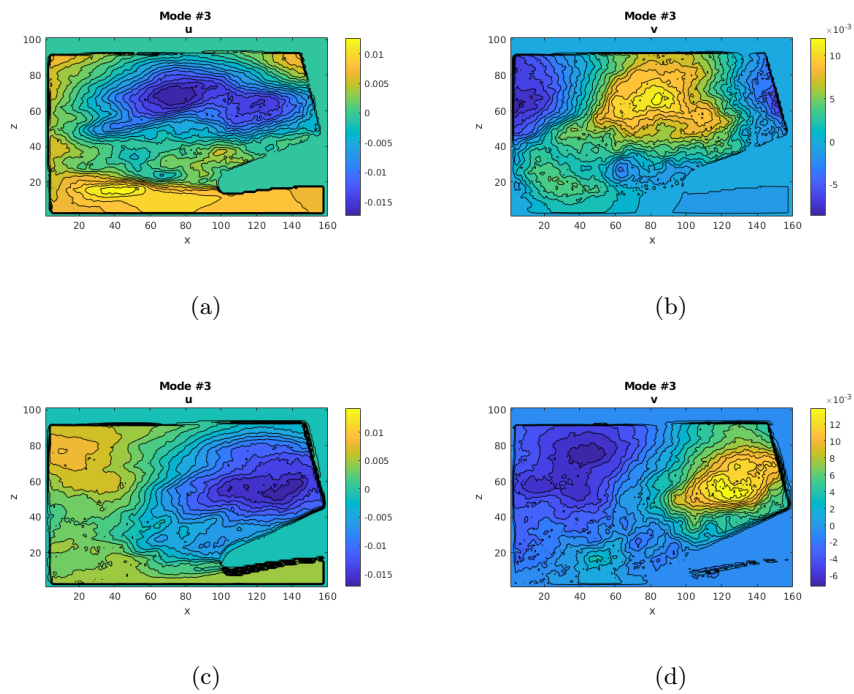


Fig. 7: (a) shows the u component of the velocity corresponding to the mode 3 while (b) shows the y component. (c) and (d) show the same corresponding to the actuated case.

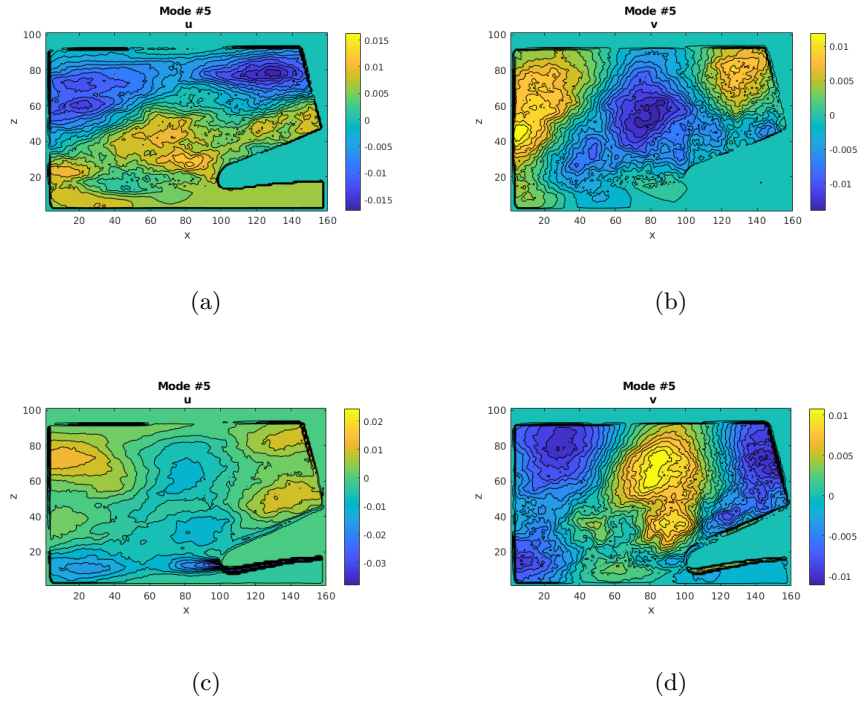


Fig. 8: (a) shows the u component of the velocity corresponding to the mode 5 while (b) shows the y component. (c) and (d) show the same corresponding to the actuated case.

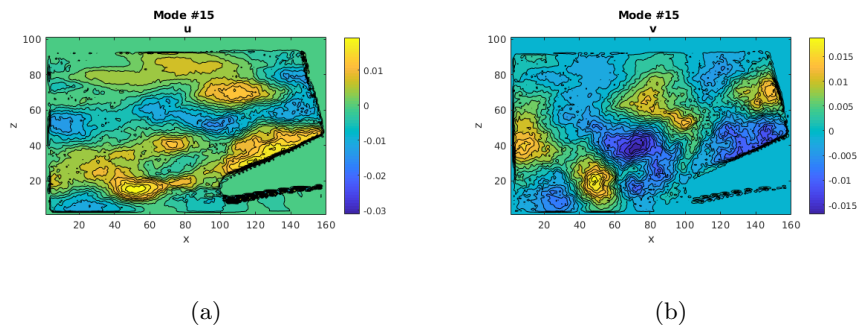


Fig. 9: Velocity components of mode 15. Cambered position.

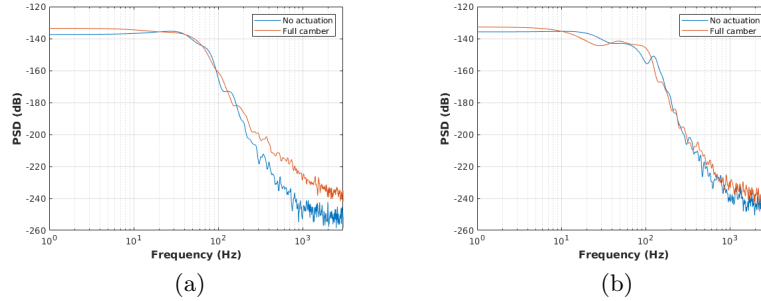


Fig. 10: Comparison between PSD of modes 3 (a) and 5 (b) in static and actuated cases.

4.2 Reconstruction from POD modes

Another possibility offered by the POD is the reconstruction of the dynamic system using a reduced number of modes. This approach allows us to identify the most energetic structures by suppressing small instabilities. Fig.11 presents the reconstruction of two different snapshots using 31 modes. Two solution times were chosen to capture both static ($t = 1.4s$) and cambered ($t = 2.36s$) configurations. The unsteady behavior of the flow in the actuated case is noticeable in both velocity components.

The flow vorticity was also calculated using 5 modes to verify the increase of the turbulence in the wake of the wing (Fig.12). Effectively, the expected result was obtained. We observe the growth of the vorticity specially inside the recirculation zone.

5 Conclusion

This paper presents the experimental study of electroactive morphing using a reduced scale prototype of an A320 wing through time-resolved PIV. As it was presented in the prototype description, the wing is embedded with two types of actuators. This work focuses in the POD analysis of the flow which shows the augmentation of wake's width caused by SMA actuation.

The influence of hybrid morphing (high and low frequency actuation at the same time) will be further investigated in the following experimental campaigns. Drag and lift measurements in the wind-tunnel are foreseen such as new PIV campaigns.

In the context of the SMS project, a closed-loop control system is intended. Through dynamic pressure sensors, the goal is to actuate the trailing edge at optimal frequencies to enhance aerodynamic performance. The results presented in this paper are promising in the sense that the variation in flow dynamics around the region where the pressure sensors are placed is quite perceptible.

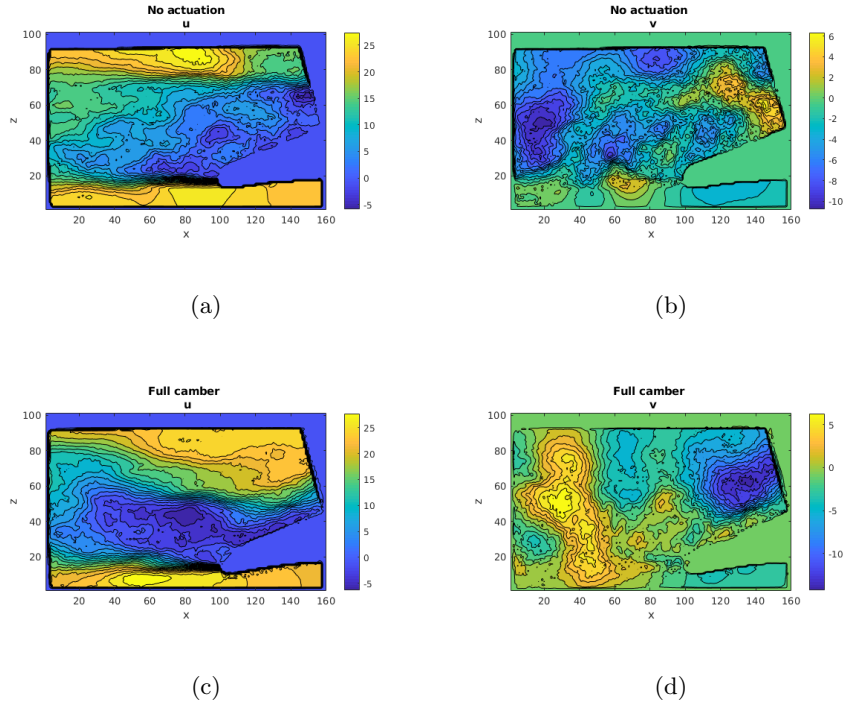


Fig. 11: Reconstruction of the flow using POD modes: (a) and (b) show the two velocity components of the static case ($t = 1.4$ seconds); (c) and (d) correspond to the full camber position ($t = 2.36$ seconds).

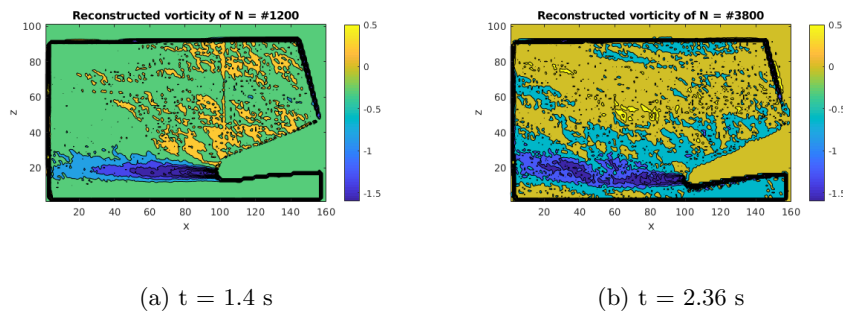


Fig. 12: Vorticity of the flow calculated from reconstructed velocity fields.

Acknowledgment

This research is part of the EU funded project: H2020 SMS Smart Morphing and Sensing for aeronautical configurations, <http://smartwing.org/SMS/EU>.

References

1. Silvestro Barbarino, Onur Bilgen, Rafic M. Ajaj, Michael I. Friswell, and Daniel J. Inman. A Review of Morphing Aircraft. *Journal of Intelligent Material Systems and Structures*, 22(9):823–877, June 2011.
2. J. C. Liao. Fish Exploiting Vortices Decrease Muscle Activity. *Science*, 302(5650):1566–1569, November 2003.
3. Ennes Sarradj, Christoph Fritzsche, and Thomas Geyer. Silent Owl Flight: Bird Flyover Noise Measurements. *AIAA Journal*, 49(4):769–779, April 2011.
4. S. Barbarino, E. I. Saavedra Flores, R. M. Ajaj, I. Dayyani, and M. I. Friswell. A review on shape memory alloys with applications to morphing aircraft. *Smart Materials and Structures*, 23(6):063001, April 2014.
5. Jean-Francois Rouchon, Dominique Harribey, Enrico Deri, and Marianna Braza. Activation d'une voilure déformable par des câbles d'AMF répartis en surface. page 6, 2011.
6. Johannes Scheller, Karl-Joseph Rizzo, Gurvan Jodin, Eric Duhayon, Jean-Francois Rouchon, and Marianna Braza. A hybrid morphing NACA4412 airfoil concept. In *2015 IEEE International Conference on Industrial Technology (ICIT)*, pages 1974–1978, Seville, March 2015. IEEE.
7. J. Scheller, M. Chinaud, JF. Rouchon, E. Duhayon, S. Cazin, M. Marchal, and M. Braza. Trailing-edge dynamics of a morphing NACA0012 aileron at high Reynolds number by high-speed PIV. *Journal of Fluids and Structures*, 55:42–51, May 2015.
8. G. Jodin, V. Motta, J. Scheller, E. Duhayon, C. Dll, J. F. Rouchon, and M. Braza. Dynamics of a hybrid morphing wing with active open loop vibrating trailing edge by time-resolved PIV and force measures. *Journal of Fluids and Structures*, 74:263–290, October 2017.
9. Gurvan Jodin, Johannes Scheller, Karl Joseph Rizzo, Eric Duhayon, Jean-Francois Rouchon, and Marianna Braza. Dimensionnement d'une maquette pour l'investigation du morphing électroactif hybride en soufflerie subsonique. In *22e Congrès Français de Mécanique (CFM 2015)*, pages 1–13, Lyon, France, August 2015.
10. Christian Lexcellent. *Shape-Memory Alloys Handbook*. John Wiley & Sons, April 2013.
11. N Simiriotis, G Jodin, A Marouf, P Elyakime, Y Hoarau, J C Hunt, and M Braza. Morphing of a supercritical wing by means of trailing edge deformation and vibration at high Reynolds numbers: experimental and numerical investigation. page 41.
12. Rodolphe Perrin. Analyse physique et modélisation d'écoulements incompressibles instationnaires turbulents autour d'un cylindre circulaire grand nombre de Reynolds. page 116.
13. Gurvan Jodin. Hybrid electroactive morphing at real scale - application to Airbus A320 wings. page 111.
14. Moritz Sieber, Kilian Oberleithner, and Christian Oliver Paschereit. Spectral proper orthogonal decomposition. *Journal of Fluid Mechanics*, 792:798–828, April 2016. arXiv: 1508.04642.